

A Quencher-Fluorophore-Type Probe for Detection and Imaging of NADPH in Human Breast Cancer Cells

Geunhyeok Yu,[†] Sungryung Kim,[†] Se Won Bae,^{‡,*} and Woon-Seok Yeo^{†,*}

[†]Department of Bioscience and Biotechnology, Bio/Molecular Informatics Center, Konkuk University, Seoul 05029, South Korea. *E-mail: wsyeo@konkuk.ac.kr

[‡]Green Chemistry and Materials Group, Korea Institute of Industrial Technology (KITECH), Cheonan 31056, South Korea. *E-mail: swbae@kitech.re.kr

Received May 10, 2019, Accepted June 7, 2019, Published online August 5, 2019

A new fluorogenic trimethyl lock quinone (TLQ) derivative, designated as the quencher-TLQ-fluorophore-type probe (Q-TLQ-F), was developed for selective detection of nicotinamide adenine dinucleotide phosphate (NADPH). By taking advantage of the well-known facile intramolecular ring cyclization reaction (δ -lactonization) of TLQ that can release a reporter molecule upon reduction, Q-TLQ-F was successfully applied for the detection of physiological NADPH generated by glucose-6-phosphate dehydrogenase in human breast cancer MDA-MB-231 cells.

Keywords: Fluorophore, Quencher, NAD(P)H, Trimethyl lock quinone, Chemosensor

Introduction

All biochemical reactions within a cell are referred to as metabolism. Cells create the polymeric materials required to generate new cells after producing energy and reducing power through metabolism.¹ Cell metabolism is divided into two categories: catabolism, which breaks down a substance, and anabolism, which synthesizes a new substance.² Catabolism is the process of decomposing and oxidizing a substrate to obtain energy and reducing power, whereas anabolism is the process of biosynthesizing a complex substance from a simple compound using the energy and reducing power obtained from catabolism.³

The key molecule responsible for the storage and release of energy is adenosine triphosphate (ATP), which transports its reducing power to nicotinamide adenine dinucleotide (NADH) and nicotinamide adenine dinucleotide phosphate (NADPH).⁴ The structure of NADPH differs slightly from that of NADH due to an additional phosphate group in the former. This phosphate group distinguishes NADPH from NADH by facilitating binding of the former to different kinds of enzymes and carriage of electrons to different targets. It plays no significant role in the transport of electrons because of its distance from the site related to electron transfer.^{5,6}

NADH and NADPH, generally referred to as NAD(P)H, participate in two different types of electron transfer reactions. NADH acts as an intermediate in catabolism for ATP generation through food oxidation. Conversely, NADPH reacts primarily with enzymes that catalyze the anabolic reactions that provide the high-energy electrons needed to synthesize biologically energetic molecules. The production of NADH in NAD⁺ and NADPH in NADP⁺ occurs through

different pathways and are regulated independently. Cells maintain a high ratio of NAD⁺ to NADH while maintaining a low ratio of NADP⁺ to NADPH.^{7,8} Thus, the abundant NAD⁺ acts as an oxidizing agent while the abundant NADPH acts as a reducing agent thereby playing distinct roles in catabolic and anabolic activities, respectively.^{9–11}

Only a limited number of studies thus far have focused on the analysis of NAD(P)H in biological samples. In the 1960s, it was reported that NAD(P)H could be detected as endogenous fluorescence signal.¹² However, this method has disadvantages such as low sensitivity and poor selectivity. Other methods commonly used since then include liquid chromatography-mass spectrometry (LC-MS) and spectrophotometer-based enzyme analysis.^{13,14} However, due to the fast turnover of NAD(P)H redox couples, quantification methods are often difficult, costly, and low-throughput. A green fluorescent protein (GFP)-based technique for imaging NAD(P)H has also been developed.^{15–17} Its mechanism of sensing depends on the conformational variation of the protein and requires intracellular gene expression. Although several other methods for NAD(P)H determination exist, including enzymatic reaction kits,¹⁸ electrochemical methods,¹⁹ and chemosensors,²⁰ they were developed to be used *in vitro* and are not suitable for cellular use.

A trimethyl lock quinone (TLQ) moiety was originally developed by modifying Cohen's model for oxidative phosphorylation.²¹ The TLQ moiety is particularly advantageous because of its facile intramolecular ring cyclization reaction (δ -lactonization) that can release a reporter molecule upon reduction.^{22–25} In this study, we focused on new TLQ reporter molecules to develop a fluorescent probe for NAD(P)H detection.

Experimental

Ninhydrin Test of TLQ-C. TLQ-C (40 μmol) in DMSO (100 μL) and a reducing agent or a control such as NaBH_4 , NADPH, NADH, NAD^+ , or NADP^+ (400 μmol , 10 equiv) in 1X PBS (900 μL) were mixed and stirred for 1 h. Ninhydrin in EtOH (100 μL , 0.08 g/mL) was then added to the reaction mixture, which was heated at 80°C for 5 min using heat blocks. After cooling to room temperature, the absorbance at 570 nm was measured using a UV spectrometer.

Fluorescence Response of Q-TLQ-F. Q-TLQ-F (0.03 mg, 24.7 nmol) was dissolved in 30 μL DMSO. NaBH_4 (123 nmol), NADPH (123 nmol), NADH (123 nmol), NADP^+ (123 nmol), glucose-6-phosphate (G6P) (0.03 mg, 123 nmol), and glucose-6-phosphate dehydrogenase (G6PD) (1.02 mU/well) were dissolved in 20 μL of PBS. Q-TLQ-F and the reagents were mixed in a well plate. The well plate was stirred for 30 min, and the fluorescence intensity of each solution was measured using a fluorescence microplate reader. The excitation wavelength was 496 nm, and the emission wavelength was 515–645 nm. The fluorescence imaging of each sample was visualized using an IVIS[®] imaging system (Caliper Life Sciences Lumina II, Hopkinton, MA, USA).

Fluorescent Cell Imaging. MDA-MB-231 cells were cultured in RPMI 1640 supplemented with 10% FBS, penicillin (100 units/mL), and streptomycin (100 $\mu\text{g}/\text{mL}$). The cells were plated in a 96-well plate and incubated for 24 h. The medium was replaced with 48 μL of HBSS and 2 μL of fluorescein solution or Q-TLQ-F solution (10 μM in DMSO). The cells were then incubated at 37°C and washed twice with HBSS. The incubation time was 30 min for fluorescein and 30 min or 1 h for Q-TLQ-F. The fluorescence images of the cells were taken using an inverted fluorescence microscope (Carl Zeiss, Oberkochen, Germany) with an EGFP filter.

Inhibitor-Dependent Fluorescence Cell Imaging. MDA-MB-231 cells were plated in a 96-well plate and incubated for 24 h. The medium was removed, and the cells were further incubated with 50 μL of DHEA (50, 100 μM in serum-free media) for 24 h at 37°C. The cell medium was then replaced with 48 μL of HHBSS and 2 μL of FQD solution (10 μM in DMSO). After 2 h at 37°C, the HHBSS and Q-TLQ-F solutions were removed, the cells washed twice using HHBSS, and the fluorescent cell images taken.

Results and Discussion

For the proof-of-concept study, we synthesized a TLQ-chloramphenicol base (TLQ-C), which is comprised of a TLQ moiety and a reporting group (chloramphenicol base and CPB) connected by an amide bond (Figure 1). The synthesis of TLQ-C was accomplished by the reported method, as shown in Figure 1(a).²⁶ Briefly, Compound (1) was activated with N-hydroxysuccinimide and coupled to a chloramphenicol base to produce TLQ-C. When TLQ-C was applied to a reducing agent, δ -lactone was formed by a

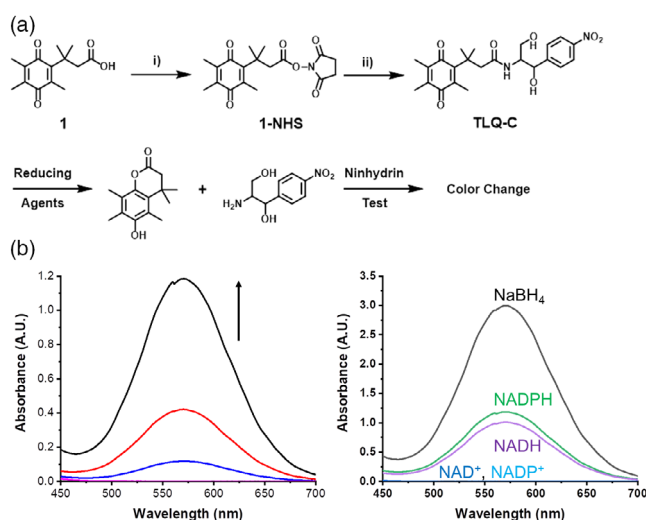


Figure 1. (a) Synthetic route and proposed detection mechanism of TLQ-C. (i) N-hydroxysuccinimide, DCC, DCM, 30 min; (ii) CPB, DIEA, DMF, 5 h. (b) UV absorption spectra of 4 mM TLQ-C with reducing agents after the ninhydrin test. Left: UV absorption spectra of TLQ-C upon addition of NADPH from 4 mM to 80 mM. Right: UV absorption spectra of TLQ-C upon addition of NaBH_4 (20 mM), NADPH (80 mM), NADH (80 mM), NAD^+ (80 mM), and NADP^+ (80 mM).

δ -lactonization reaction, and the reporting group (CPB) was subsequently released. CPB was used to detect the color change through the ninhydrin test after δ -lactonization. The most intense color change was observed with NaBH_4 , which was the strongest reducing agent screened (Figure 1(b)). The TLQ-C containing a trimethyl lock derivative with an amide bond, along with CPB, produced ninhydrin-active signals with NaBH_4 and NAD(P)H, but no color change was observed with NAD^+ and NADP^+ .

Next, we designed a fluorescent sensing system, designated as the quencher-TLQ-fluorophore-type probe (Q-TLQ-F), to sense NADPH. Q-TLQ-F was comprised of a TLQ and a fluorescein linked by an amide bond (Figure 2). Moreover, Q-TLQ-F contained a quencher moiety to efficiently absorb the fluorescence of a fluorescein moiety. For detailed synthetic schemes and experimental procedures for TLQ-C and Q-TLQ-F, see Supporting Information. The fluorescence response of Q-TLQ-F with reducing agents was investigated. The concentrations of the reducing agents were well below 1 mM, similar to what is observed under normal biological conditions. As shown in Figure 2(b), the fluorescence intensity of Q-TLQ-F (0.5 mM) gradually increased and became saturated after incubation with up to 5 equiv of NADPH for 150 min at 519 nm, whereas it took less than 10 min to observe the quick saturation of fluorescence with NaBH_4 . The higher (nearly five times) green fluorescence emission indicated that Q-TLQ-F was reduced by the reducing agents (NaBH_4 and NADPH) followed by the removal of a fluorescein from the quencher moiety.

Prior to the examination of Q-TLQ-F as a turn-on fluorescent probe for the in-cell detection of NADPH, its sensing

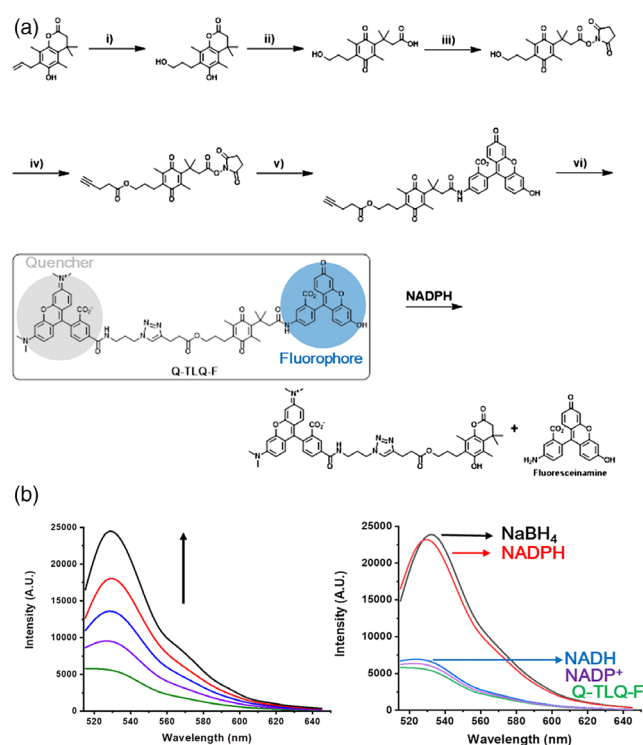


Figure 2. (a) Synthetic route and proposed detection mechanism of Q-TLQ-F. (i) BH₃, THF, N₂, then NaOH, H₂O₂; (ii) NBS, MeCN/DI water; (iii) EDC, NHS, DCM; (iv) 4-pentynoic acid, DCC, DMAP, DCM; (v) aminofluorescein, DIEA, DCM/DMSO; (vi) TAMRA-N₃, copper(I) acetate, DMSO. (b) Left: Fluorescence enhancement of Q-TLQ-F (0.5 mM) with 5 equiv of NADPH over an incubation time of 0, 10, 20, 60, 150 min ($\lambda_{\text{ex}} = 496$ nm). Right: Fluorescence response of Q-TLQ-F (0.5 mM) co-incubated with 5 equiv of various reducing agents for 150 min ($\lambda_{\text{ex}} = 496$ nm).

ability for the detection of physiological NADPH was investigated. Figure 3(a) represents an early stage of the pentose phosphate pathway (PPP).²⁷ The enzyme glucose-6-phosphate dehydrogenase (G6PD) converts glucose 6-phosphate (G6P) with NADP⁺ to 6-phosphogluconolactone (d-6PGL) and NADPH in cells. We examined whether Q-TLQ-F could sense the NADPH generated by G6PD (Figure 3(b) and (c)). When Q-TLQ-F was applied to NaBH₄ (entry 1) and NADPH (entry 2), a strong fluorescence signal was emitted. Q-TLQ-F also showed a strong fluorescence intensity for NADPH produced by G6PD (entry 6), which corresponded to the results shown in entries 1 and 2. As a control, only a weak fluorescence signal in the presence of NADH (entry 3) or in the absence of G6PD (entry 4) and NADP⁺ (entry 5) was observed. Thus, we confirmed that Q-TLQ-F could detect physiological NADPH generated by G6PD with an increased level of fluorescence and could be used as a sensor to measure the activity of G6PD.

We also carried out a cell fluorescence imaging experiment to investigate the potential applications of Q-TLQ-F. For this purpose, human breast cancer MDA-MB-231 cells were treated with Q-TLQ-F (2 μ L and 10 μ M) and

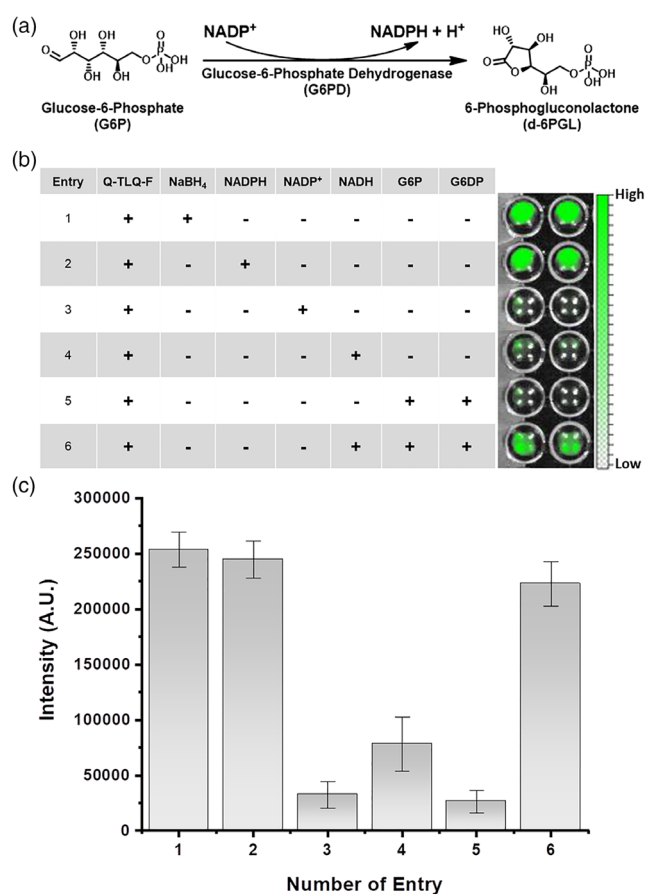


Figure 3. (a) Early stage of the pentose phosphate pathway (PPP). (b) Fluorescence response of Q-TLQ-F (0.5 mM) co-incubated with 5 equiv of various biological reducing agents (2.5 mM) in PBS buffer for 30 min ($\lambda_{\text{ex}} = 496$ nm). (c) Average fluorescence intensity of each entry.

incubated at 37°C. After incubation, the cells were washed twice with Hank's balanced salt solution (HBSS) and fluorescence microscopy images were obtained. Figure 4 reveals that Q-TLQ-F is taken up and transformed into a δ -lactone and a fluorescein in the cells. After 30 min of incubation, only trace fluorescence was observed. However, most cells displayed a high intensity of green fluorescence after 1 h of incubation, verifying that Q-TLQ-F has the ability to detect intracellular NADPH as a turn-on fluorescence system.

The activity of Q-TLQ-F was further confirmed by investigating inhibitor-dependent NADPH production. Dehydroandrosterone (DHEA), an abundantly produced adrenal steroid, is an uncompetitive inhibitor of mammalian G6PD that decreases cellular NADPH levels.²⁸ The fluorescence microscopy images of the MDA-MB-231 cells treated with DHEA for 30 min, followed by Q-TLQ-F incubation, showed only minimal fluorescence (Figure 5). In the presence of the inhibitor, the fluorescence levels of the cells decreased with increasing inhibitor concentration. Without DHEA treatment, however, the cells displayed a bright fluorescence as expected. This

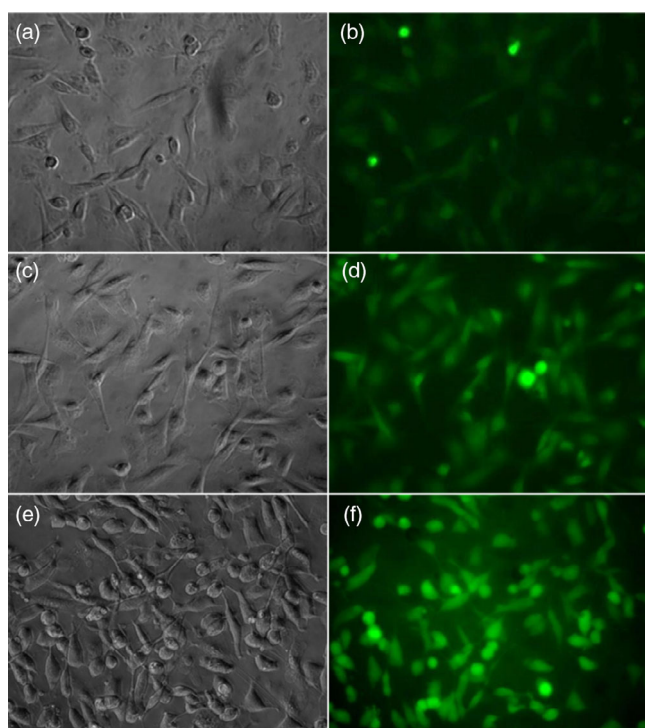


Figure 4. Fluorescence microscopy images of MDA-MB-231 cells taken after incubation for (a, b) 30 min, (c, d) 60 min, and (e, f) 120 min with Q-TLQ-F (2 μ L, 10 μ M) using an inverted fluorescence microscope (Carl Zeiss) with an EGFP filter.

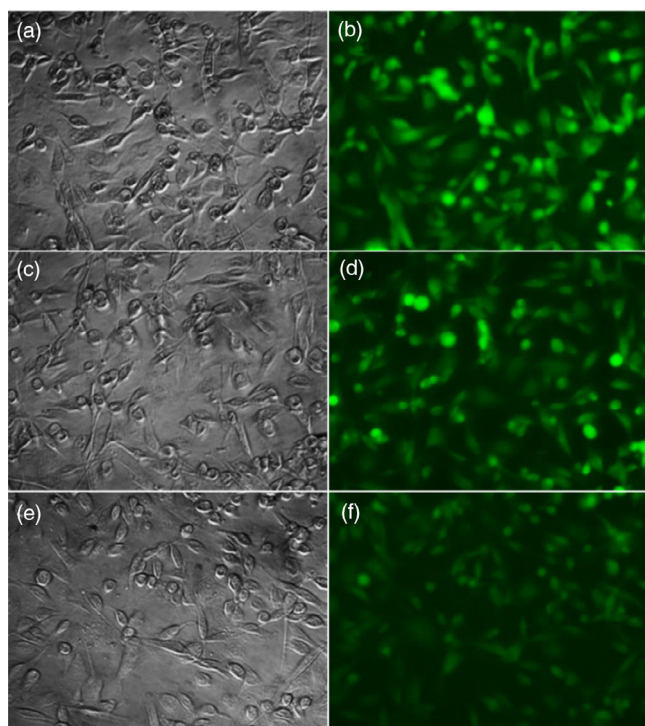


Figure 5. Fluorescence microscopy images of MDA-MB-231 cells taken after incubation with 50 μ L of (a, b) 0 μ M, (c, d) 50 μ M, and (e, f) 100 μ M DHEA for 24 h followed by incubation with 2 μ L of Q-TLQ-F (10 μ M) for 2 h using an inverted fluorescence microscope with an EGFP filter.

result indicates that Q-TLQ-F responded to the NADPH level that was modulated by G6PD inhibition in the cells.

Conclusion

In this study, a quencher-fluorophore-type probe, Q-TLQ-F, was developed for the intracellular detection and imaging of NADPH in human breast cancer cells (MDA-MB-231). Q-TLQ-F selectively responded to NADPH under physiological conditions. FQD was also used for the fluorescence imaging of MDA-MB-231 cells. We are presently working on a follow-up study to find the source of Q-TLQ-F that selectively responds to NADPH and weakly responds to NADH.

Acknowledgments. This research was supported by Basic Science Research Program (NRF-2016R1D1A1A09918111) through the National Research Foundation of Korea (NRF) funded by the Ministry of Education and by the Big Issue Program funded by the KITECH, Republic of Korea (Project No. EO190029).

Supporting Information. Additional supporting information may be found online in the Supporting Information section at the end of the article.

References

1. B. Alberts, D. Bray, J. Lewis, M. Raff, K. Roberts, J. D. Watson, *Molecular Biology of the Cell*, 3rd ed., Garland Publishing, Inc, New York, **1994**.
2. J. M. Berg, J. L. Tyymoczko, L. Stryer, *Biochemistry*, 5th ed., W. H. Freeman and Company, New York, **1995**.
3. R. J. DeBerardinis, C. B. Thompson, *Cell* **2012**, *148*, 1132.
4. M. Bonora, S. Patergnani, A. Rimessi, E. D. Marchi, J. M. Suski, A. Bononi, C. Giorgi, S. Marchi, S. Missiroli, F. Poletti, M. R. Wieckowski, P. Pinton, *Purinergic Signal* **2012**, *8*, 343.
5. F. Berger, M. H. Ramirez-Hernandez, M. Ziegler, *Trends Biochem. Sci.* **2004**, *29*, 111.
6. (a) W. Ying, *Front. Biosci.* **2006**, *11*, 3129. (b) M. Ziegler, *Eur. J. Biochem.* **2000**, *267*, 1550.
7. H. B. Burch, M. E. Bradley, O. H. Lowry, *J. Biol. Chem.* **1967**, *242*, 4546.
8. R. L. Veech, L. V. Eggleston, H. A. Krebs, *Biochem. J.* **1969**, *115*, 609.
9. N. Pollak, C. Dolle, M. Ziegler, *Biochem. J.* **2007**, *402*, 205.
10. N. Pollak, M. Niere, M. Ziegler, *J. Biol. Chem.* **2007**, *282*, 33562.
11. J. Park, J. J. Chung, J. B. Kim, *Diabetes Res. Clin. Pract.* **2007**, *77*, 11.
12. O. H. Lowry, J. V. Passonneau, M. K. Rock, *J. Biol. Chem.* **1961**, *236*, 2756.
13. R. G. Kerr, K. Kelly, *J. Nat. Prod.* **1999**, *62*, 201.
14. V. B. Ritov, E. V. Menshikova, D. E. Kelley, *Anal. Biochem.* **2004**, *333*, 27.
15. Y. Zhao, A. Wang, Y. Zou, N. Su, J. Loscalzo, Y. Yang, *Nat. Protoc.* **2016**, *11*, 1345.
16. Y. Zhao, Y. Yang, *Free Radic. Biol. Med.* **2016**, *100*, 43.

17. R. Tao, Y. Zhao, H. Chu, A. Wang, J. Zhu, X. Chen, Y. Zou, M. Shi, R. Liu, N. Su, J. Du, H. M. Zhou, L. Zhu, X. Qian, H. Liu, J. Loscalzo, Y. Yang, *Nat. Methods* **2017**, *14*, 720.
 18. J. A. Khan, F. Forouhar, X. Tao, L. Tong, *Expert Opin. Ther. Targets* **2007**, *11*, 695.
 19. S. Han, T. Du, H. Jiang, X. Wang, *Biosens. Bioelectron.* **2017**, *89*, 422.
 20. H. Ito, T. Terai, K. Hanaoka, T. Ueno, T. Komatsu, T. Nagano, Y. Urano, *Chem. Commun.* **2015**, *51*, 8319.
 21. J. W. Thanassi, L. A. Cohen, *Biochim. Biophys. Acta Bioenerg.* **1969**, *172*, 389.
 22. H. Seo, I. Choi, J. Lee, S. Kim, D.-E. Kim, S. K. Kim, W.-S. Yeo, *Chem. Eur. J.* **2011**, *17*, 5804.
 23. J. Lee, I. Choi, W.-S. Yeo, *Chem. Eur. J.* **2013**, *19*, 5609.
 24. Y. Zheng, B. Yu, K. Ji, Z. Pan, V. Chittavong, B. Wang, *Angew. Chem. Int. Ed.* **2016**, *55*, 4514.
 25. I. Choi, S. W. Bae, W.-S. Yeo, *Bull. Kor. Chem. Soc.* **2017**, *38*, 296.
 26. L. Carpino, S. Triolo, R. Berglund, *J. Org. Chem.* **1989**, *54*, 3303.
 27. N. J. Kruger, A. von Schaewen, *Curr. Opin. Plant Biol.* **2003**, *6*, 236.
 28. M. D. Monaco, A. Pizzini, V. Gatto, L. Leonardi, M. Gallo, E. Brignardello, G. Boccuzzi, *Br. J. Cancer* **1997**, *75*, 589.
-